Macromolecules

ARTICLE

pubs.acs.org/Macromolecules

Mechanically and Thermally Enhanced Intrinsically Dopable Polyimide Membrane with Advanced Gas Separation Capabilities

Chang-Jian Weng,[†] Yu-Sian Jhuo,[†] Kuan-Yeh Huang,[‡] Chun-Fang Feng,[†] Jui-Ming Yeh,[†,*] Yen Wei,[§] and Mei-Hui Tsai[∥]

[†]Department of Chemistry and Center for Nanotechnology, Chung-Yuan Christian University, Chung Li 32023, Taiwan, R.O.C

[‡]Material and Chemical Research Laboratories, Industrial Technology Research Institute, Hsin Chu 310, Taiwan, R.O.C

[§]Department of Chemistry, Drexel University, Philadelphia, Pennsylvania 19104, United States

[∥]Department of Chemical and Materials Engineering, Chin-Yi Institute of Technology, Taichung 41111, Taiwan, R.O.C

Supporting Information

ABSTRACT: In this paper, we present the first preparation of an intrinsically dopable polyimide (DPI) membrane containing an amine-capped aniline trimer (ACAT) that reveals advanced gas separation capabilities as well as mechanically and thermally enhanced properties. The as-prepared DPI membrane was synthesized by reacting ACAT and 4,4′-(4,4′-isopropylidenediphenoxy)bis(phthalic anhydride) (BSAA) through a conventional thermal imidization reaction. Polyaniline (PANI) and conventional nondopable polyimide (NDPI) membranes were also prepared as controls. The DPI membranes were found to reveal permselectivities (α) of O_2/N_2 of about 13.54, which is about 1.96- and 1.54-fold higher than that of NDPI and PANI, respectively, based on the investigation of gas permeability analysis (GPA). Upon doping with 1.0 M HCl (aq), the pemselectivities of DPI for O_2/N_2 were found to be further increased to about 16.63. Moreover, significantly enhanced mechanical and thermal properties of the as-prepared DPI membrane were also found as compared to those of NDPI and PANI membranes, based on the studies of dynamic mechanical analysis (DMA) and thermogravimetric analysis (TGA), respectively.

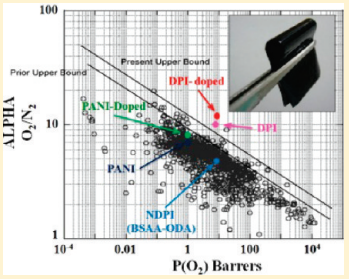

INTRODUCTION

Membrane science and technology are recognized today as powerful tools in solving some important global problems, such as developing new processes needed for sustainable industrial growth. The key for new applications of membranes in challenging and harsh environments (e.g., petrochemistry) lies in the development of new, tough, high performance materials. To develop good gas separation membrane materials, it is important to investigate the factors influencing gas permeability, permselectivity, thermal stability, and mechanical properties of polymers.

A number of reviews examining the various materials for gas separation membranes have been published over the last two decades.[1−10] Among the studied materials, it was noted that polyimides (PI), which exhibit high permselectivity for various gas pairs (e.g., CO_2/CH_4 and O_2/N_2), high chemical resistance, thermal stability, and mechanical strength, have attracted much attention. To the best of our knowledge, there are about 450 publications related to gas separation studies of polyimide membranes in the ISI web database.

Gas separation studies associated with polyaniline (PANI) membranes were first initiated by Anderson et al. in early 1990.[11,12] Research interest in using PANI also lies in the fact that film morphology can be modified after synthesis by a convenient doping process, which enables the optimization of a particular separation. In contrast, controlling the morphology of a polymer after its synthesis is difficult to accomplish with conventional polymers such as polyimide since they cannot readily be intrinsically doped. Therefore, some research groups have attempted to control the morphology of a polyimide membrane in order to fine-tune the gas separation by blending different feeding ratios of PANI.[13−15]

Recently, research activities in terms of oligoanilines with well-defined structures for modeling the electronic, magnetic, and optical properties of PANI have been evoked.[16,17] Moreover, electroactive polymers derived from oligoaniline, such as electroactive polyimide,[18−20] electroactive polyamide,[20−23] and electroactive epoxy,[24,25] have also attracted considerable research interest. However, to the best of our knowledge, reports on gas separation studies using electroactive polyimide membranes are limited. In this paper, therefore, we present the first preparation of an intrinsically dopable polyimide (DPI) membrane and investigate its advanced gas separation capabilities using gas permeability analysis (GPA), followed by an evaluation of the mechanical strength and thermal stability of the corresponding membrane by dynamic mechanical analysis (DMA) and thermogravimetric analysis (TGA), respectively.

Received: May 17, 2011
Revised: June 26, 2011
Published: July 11, 2011

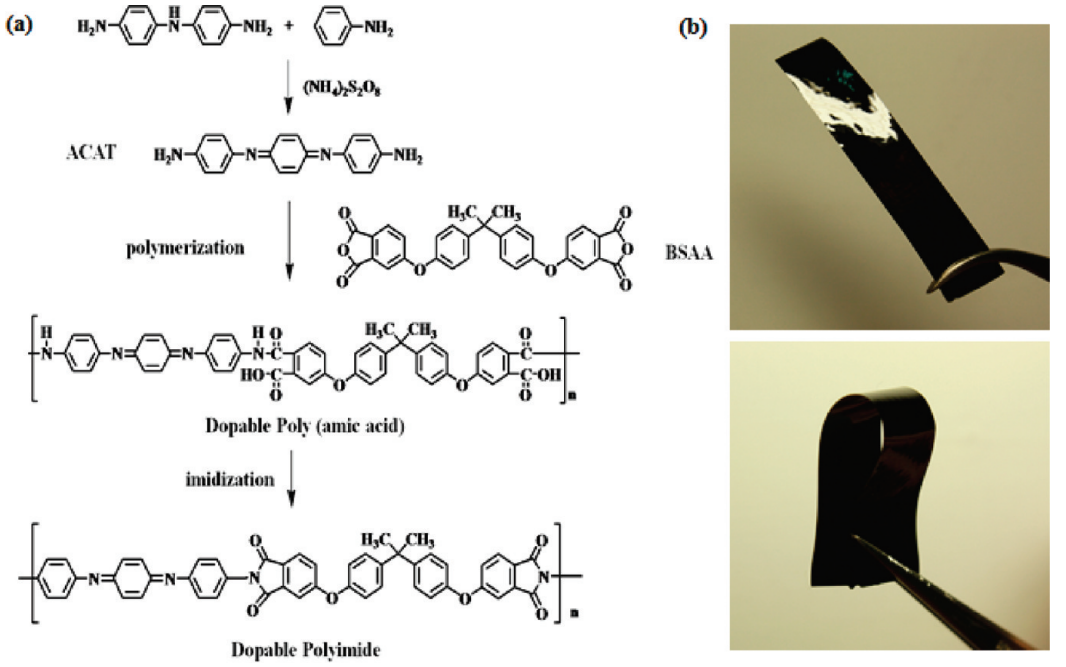

Figure 1. (a) Schematic representation of the synthesis of ACAT and dopable polyimide (DPI) and (b) photographs of DPI.

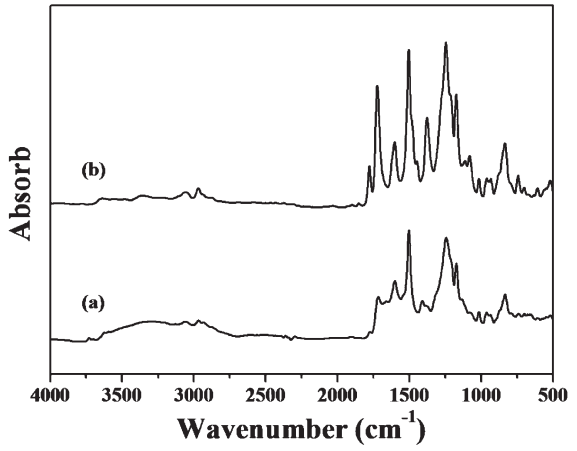

Figure 2. FTIR spectra of the obtained (a) DPAA and (b) DPI without additional dopant.

EXPERIMENTAL SECTION

Chemicals and Instrumentation. Aniline (Sigma-Aldrich) was distilled prior to use. The compounds 4,4′-oxidianiline (ODA; Fluka, Buchs, Switzerland), 1,4-phenylenediamine (Sigma-Aldrich), *N*,*N*-dimethylacetamide (DMAc, Mallinckrodt/Baker, Paris, KY), 4,4′-(4,4′-isopropylidenediphenoxy)bis(phthalic anhydride) (BSAA, Sigma-Aldrich, 97%) and sodium chloride (NaCl, Sigma-Aldrich) were used as received without further purification. All the reagents were reagent grade unless otherwise stated.

Attenuated total reflectance FTIR was obtained with an FTIR spectrometer (JASCO FTIR-4100) at room temperature. Electroactive experiments were performed using a VoltaLab 40 (PGZ 301) analytical voltammeter with a conventional three-electrode system. A Yanagimoto Co., Ltd. gas permeability analyzer

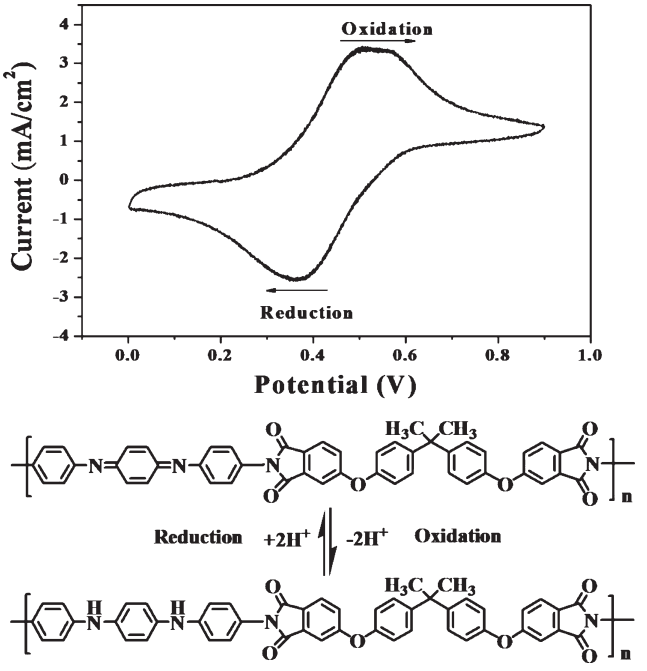

Figure 3. Cyclic voltammetry of the DPI membranes measured in aqueous H_2SO_4 (1.0 M) at a scan rate of 50 mV s^{-1}.

(model GTR31) was employed to perform the permeation experiment for oxygen/nitrogen and carbon dioxide/methane gases. Dynamic mechanical analysis (DMA) measurements were made using a TA Instruments DMA Q 800 at a heating rate of 3 °C/min from 30 to 350 °C and a frequency of 1 Hz. The thermal stabilities of all the samples were characterized by thermal gravimetric analysis (TGA). TGA scans were performed under air flow using a TA Q50 at a heating rate of 10 °C/min.

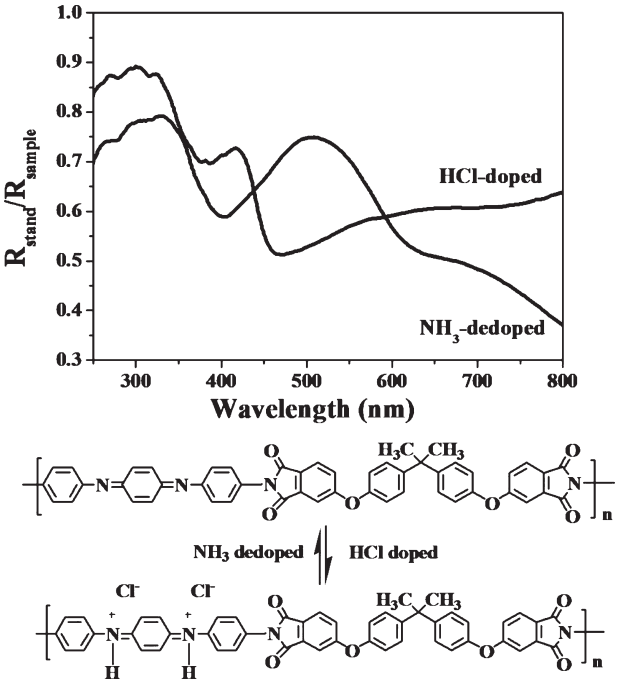

Figure 4. UV−vis spectra of the corresponding DPI membrane.

Wide-angle X-ray diffraction (WAXD) study of the samples was performed on a Rigaku D/MAX-3COD-2988N X-ray diffractometer with copper target and Ni filter at a scanning rate 2°/min. Energy-dispersive X-ray (EDX) spectroscopy image of chloride element mapping was recorded on a HITACHI-S-4100 microscopy.

Synthesis of *N,N′*-Bis(4′-aminophenyl)-1,4-quinonenediimine (ACAT). The compounds 4,4′-diaminodiphenylamine sulfate (23.65 g, 0.796 mol) and aniline (7.40 g, 0.796 mol) were dissolved in aqueous HCl solution (1.0 M, 800 mL) containing 75 g of NaCl. A solution of ammonium persulfate (18.00 g, 0.789 mol) in aqueous HCl (1.0 M, 200 mL) was added via a dropping funnel into the above solution at −5 °C at a rate of approximately 60 drops/min. The reaction mixture was stirred for 1 h at −5 °C. The resulting precipitate was collected by filtration and washed with aqueous HCl solution (1.0 M, 400 mL) which was precooled to 0 °C. The solid product was washed with 1 M NH_4OH solution (100 mL) and a large amount of distilled water and then dried in a vacuum oven at 50 °C overnight. The amine-capped aniline trimer (ACAT) was obtained as a blue solid. 11.8 g (51.5%). ^{1}H NMR (300 MHz, DMSO-d_6): δ 6.95 (s, 4H), 6.80−6.60 (dd, 8H), 5.42 (s, 4H). MS (ESI) calcd for $C_{18}H_{16}N_4$ [M]: 288.14. Found: 289.1 $[M + H]^+$.

Synthesis of Dopable Polyimide (DPI). Dopable polyimide (DPI) and nondopable polyimide (NDPI) were prepared using either *N,N′*-bis(4′-aminophenyl)-l,4-quinonenediimine (ACAT) or 4,4′-oxidianiline (ODA) as a diamine and 4,4′-(4,4′-isopropylidenediphenoxy)bis(phthalic anhydride) (BSAA) as a dianhydride. A typical procedure o prepare the free-standing DPI membrane or NDPI membrane was as follows: BSAA (1.04 g, 2 mmol) was added to 6.0 g of DMAc at room temperature with continuous stirring for 30 min. A separate solution containing ACAT (0.578 g, 2 mmol) or ODA (0.400 g, 2 mmol) in another 6 g of DMAc was prepared under magnetic stirring. After stirring for 30 min, both solutions were mixed together. The as-prepared mixture was then stirred for an additional 3 h at room temperature. It was subsequently poured onto the supporting substrate to form the DPI film and then dried under vacuum at 250 °C for 2 h. The procedure for synthesizing the free-standing DPI film is depicted in Figure 1(a). ^{1}H NMR(300 MHz, DMSO-d_6, δ, ppm): 1.38 (s, 18H, $-CH_3$), 6.6−7.5 (m, 12H, $H_b + H_d + H_e + H_f + H_g + H_h$), 7.7−8.1(m, 6H, $H_a + H_c$).

Synthesis of Polyaniline. An aniline monomer (0.1 mol) was subsequently added to H_2O and the resulting solution was stirred for another 1 h. Upon addition of ammonium persulfate (0.025 mol) in 20 mL of 1.0 M HCl (aq), the solution was stirred for 3 h at −5 °C in an ice bath. The as-synthesized HCl-doped precipitates were then obtained by filtering and drying under dynamic vacuum at room temperature for 48 h. The final PANI products in base form were obtained by immersing the HCl-doped precipitates in 400 mL of 1.0 M NH_4OH (aq) and magnetically stirring for 4 h at room temperature, followed by filtration and drying under vacuum at room temperature for 48 h. The polyaniline membrane preparation is given as follows: 0.3 g of as-prepared sample was introduced into 10 mL of NMP solution under magnetic stirring for 24 h at room temperature.

Gas Permeation Study. A gas permeation analyzer (Yanaco GTR 31) was used to measure the mixed gas permeability coefficients, *P*, for the membranes. The gas transport properties for DPI, NDPI, and PANI membranes were evaluated from thin films having a nominal thickness of 50 μm. Gases employed in this study included O_2, N_2, and CO_2, and all of which were 99.999% pure. An absolute feed pressure of 3 atm was used in all permeation tests at 303, 313, 323, and 333 K. The permeability unit is usually expressed in barrer [one barrer $=10^{-10}$ (cm^3 (STP) cm)/(cm^2 s cmHg)]. The gas permselectivity was calculated from the ratio of permeability of different gases, which is defined as follows: $\alpha_{A/B} = P_A/P_B$, where P_A and P_B are the permeability of gases A and B, respectively.

RESULTS AND DISCUSSION

Intrinsically dopable polyimide (DPI) membrane was prepared by reacting a conjugated diamine of amine-capped aniline trimer (ACAT) with a nonconjugated dianhydride of BSAA through conventional chemical imidization reactions. A typical flowchart for the preparation of DPI is shown in Figure 1a. The as-prepared DPI membrane with membrane thickness of 50 μm and exhibiting a shiny surface was found to exhibit toughness and flexibility simultaneously, as shown in Figure 1b.

Figure 2 shows the FTIR spectra of obtained intrinsically (a) dopable polyamic acid (DPAA) membranes and (b) DPI membranes without dopant. For example, the characteristic absorption bands appearing at 3300 and 3200 cm^{-1} were assigned to be the terminal $-NH_2$ molecules of ACAT. The characteristic absorption peaks found at 1600 and 1500 cm^{-1} were attributed to the characteristic vibration bands of the quinoid and benzenoid rings of ACAT, respectively.[20,25,26] The absorption peak located at 830 cm^{-1} was determined to be a characteristic of the *para*-substitution of the 1,4-disubstituted benzene ring. An obvious peak found at 3405 cm^{-1} was attributed to the vibration band of N−H stretching. Moreover, the vibration bands appearing at around 1778 and 1720 cm^{-1} resulted from the asymmetric and symmetric carbonyl stretching of imide groups. The characteristic peak occurred at 1346 cm^{-1} could be assigned to the vibrational band of C−N stretching that arose from secondary aromatic amine groups. The representative peak found at 1170 cm^{-1} resulted from the stretching mode of N═Q═N (Q is quinoid ring).[18,24]

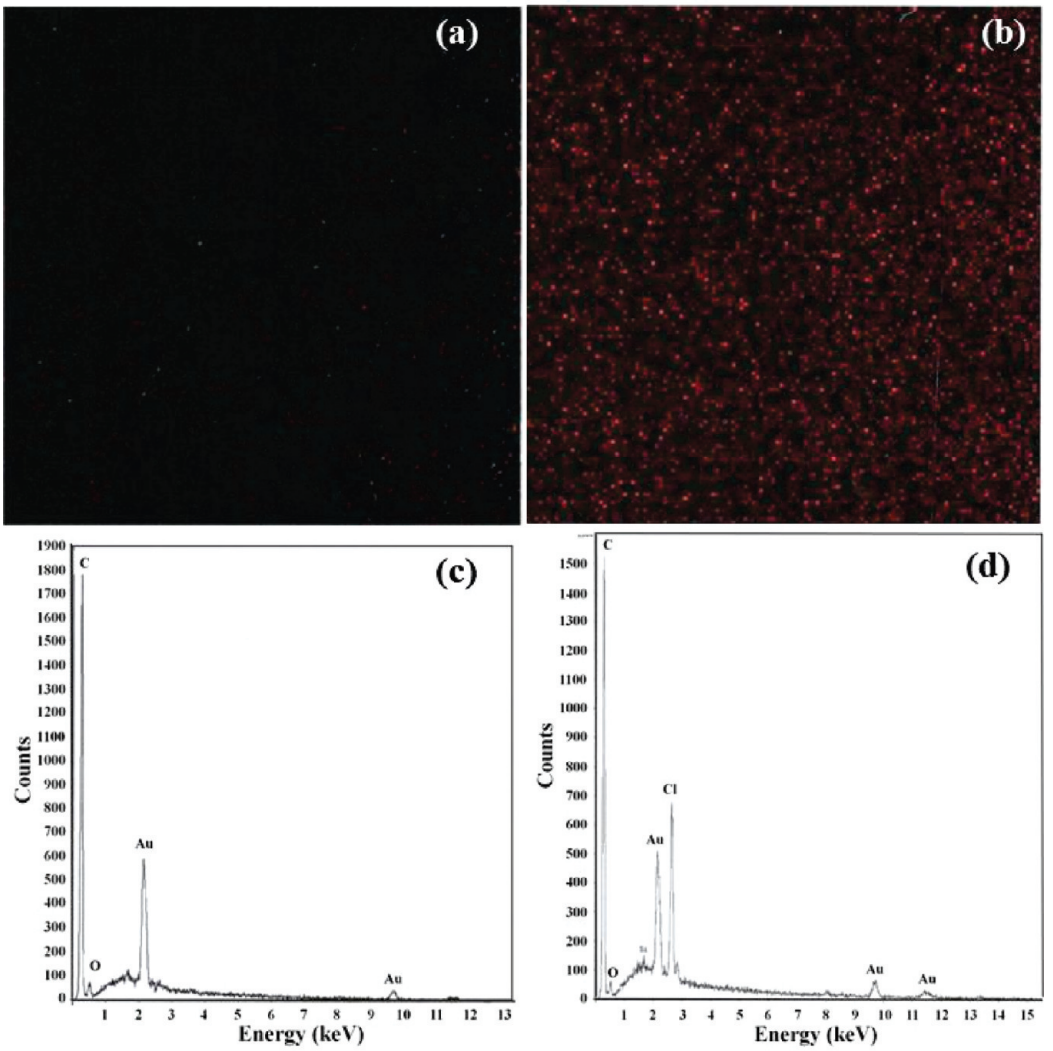

Figure 5. SEM Cl-mapping on (a) DPI and (b) DPI-doped; EDX—element distribution for (c) DPI and (d) DPI-doped.

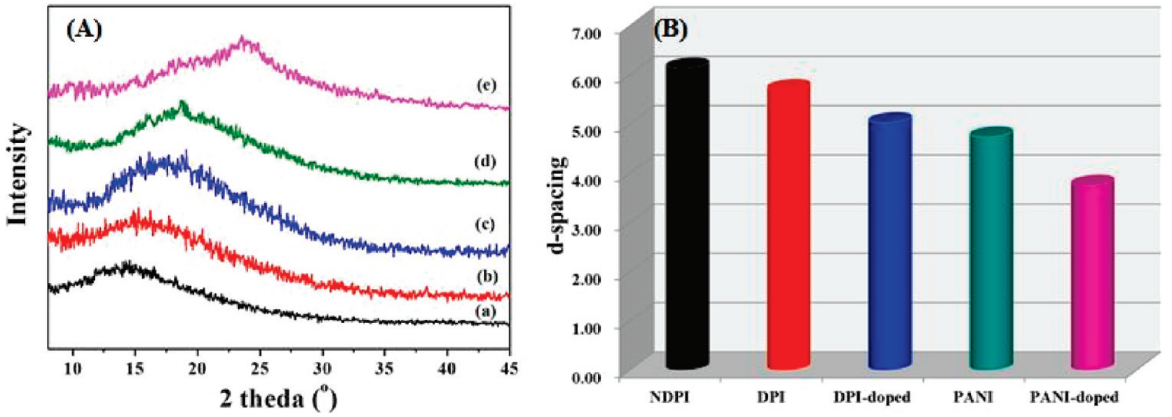

Figure 6. (A) X-ray diffraction patterns of (a) NDPI, (b) DPI, (c) DPI-doped with 1 M HCl, (d) PANI, and (e) PANI-doped with 1 M HCl. (B) *d*-space values with all samples.

A characteristic peak associated with the out-of-plane C—H bending existing in the 1,4-disubstituted benzene ring was reflected at 830 cm^{-1}. A characteristic peak near 740 cm^{-1} due to the imide ring deformation[26] of DPI was also found in the FTIR spectra.

According to the proposed mechanism for electrochemical redox reaction of aniline oligomers,[27] the electrochemical behavior of the obtained DPI membranes was examined in a strongly acidic electrolyte composed of 1.0 M H_2SO_4 aqueous solution. DPI was formed by coating DPAA on the surface of a Pt working electrode, followed by thermal imidization into DPI. Figure 3 shows the cyclic voltammetry (CV) of the DPI obtained using a saturated calomel electrode (SCE) as the reference electrode with a scan rate of 50 mV s^{-1}. Under these conditions, CV studies of the DPI membrane showed a pair of reversible redox peak, which was similar to many longer oligomers that undergo a two-electron-transfer process.[28] For the studies of DPI, a single oxidation peak was found to occur at a lower potential of 582 mV as compared to that of PANI at a potential of 800 mV. We envisioned that the oxidation peak shift of DPI as compared to that of PANI could be attributed to the transition of DPI from a reduced state to an oxidized state.

Table 1. Physical Properties of NDPI, DPI, DPI-Doped, PANI, and PANI-Doped Membranes

compound code	2θ (deg)	d-spacing (Å)	ρ(g/cm^3)	FFV
NDPI	14.44	6.13	1.268	0.152
DPI	15.56	5.69	1.283	0.133
DPI-doped	17.65	5.02	1.313	0.112
PANI	18.73	4.73	1.258	0.090
PANI-doped	23.68	3.75	1.320	0.056

Upon doping with HCl, the corresponding electrical conductivity of DPI membranes was also found to change, as demonstrated by the diffuse reflectance UV−visible spectrum by using an integrating sphere and $BaSO_4$ as a white standard. Diffuse reflectance spectrum were recorded as R_{stand}/R_{sample} versus wavelength, where R is the absolute reflection intensity (Figure 4). Similar to PANI, the quinoid (Q) absorption peak appearing at 509 nm and the benzenoid (B) peak located at 312 nm were assigned to two characteristic peaks existing in the emeraldine base (EB) form of DPI. These peaks were associated with the transition of $\pi_b-\pi_q$ from a benzene unit to a quinone unit and from the $\pi-\pi^*$ transition in the benzene unit, respectively.[29,30] Moreover, the emeraldine salt (ES) form of DPI could be generated upon doping with HCl. It should be noted that the two electronic transitions found at 312 and 509 nm gradually disappeared upon doping with HCl; instead, new bands were observed at around 415 and 800 nm. The peak appearing at 415 nm was probably due to the formation of polarons (radical cations) caused by the electron transition of quinoid to benzoid units. The peak found at 800 nm with a long tail was assigned to the polaron transition, which typically characterizes protonation[31] and is identical to that of the emeraldine salt (ES) form of the DPI membrane.

The effectiveness of the doping process in the DPI polymer matrix was also studied using an SEM mapping technique. Figure 5 shows SEM mapping and energy dispersive X-ray (EDX) spectra of the surfaces of the DPI and DPI doped with 1 M HCl (aq).

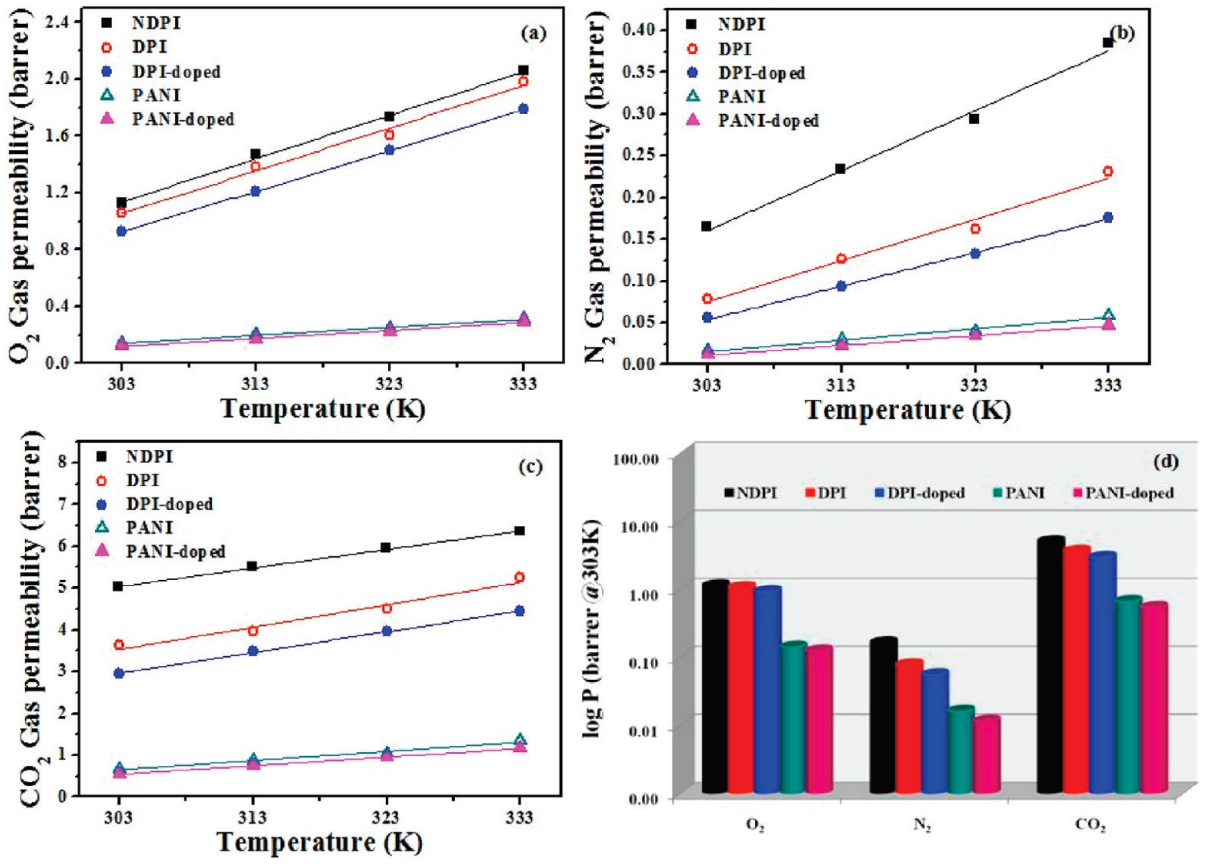

Figure 7. Variation of permeability coefficient for the studied membranes with temperature−mixed air gases: (a) O_2, (b) N_2 and pure gases, and (c) CO_2 at 1 barrer. (d) Variation of permeability coefficient for membranes at 303 K.

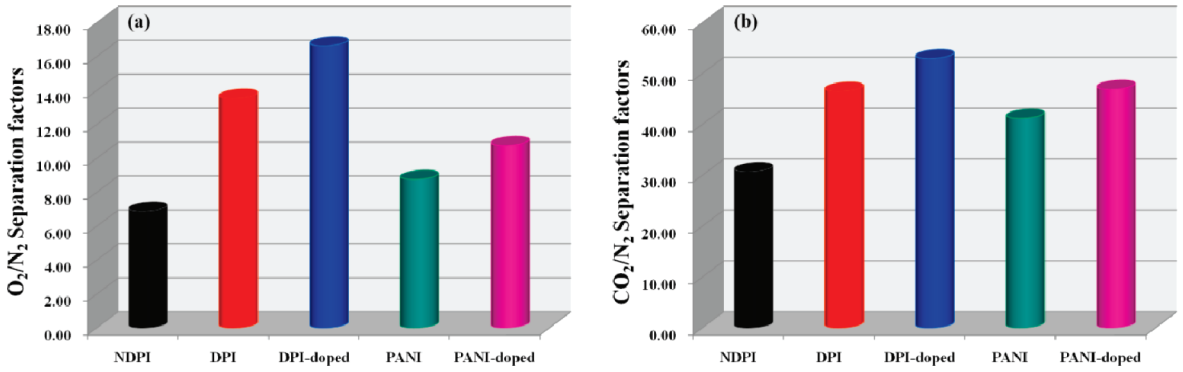

Figure 8. Variation of permeability selectivity for the studied membranes at 303 K (a) O_2/N_2 and (b) CO_2/N_2.

Table 2. Comparison of Permeability of O_2 and Selectivity Factor of O_2/N_2 Data Appearing in the Literature

kind of materials	membranes	researcher	$P(O_2)$	O_2/N_2	ref
polyaniline (PANI)	PANI	Anderson et al. (1991)	0.1	6.66	11, 37
	PANI	Wang et al. (1999)*	0.151	9.15	38
	PANI	Young Moo Lee (1999)	0.49	7.2	39
	PANI-doped	Young Moo Lee (1999)	0		39
	PANI	Min-Jong Chang (1996)	0.12	7.06	40
	PANI-doped	Min-Jong Chang (1996)	0.016	–	41
	PANI	Rebattet et al. (1995)*	0.121	6.36	41
	PANI-doped	Rebattet et al. (1995)*	0.01	2.5	41
	PANI- doped	Martin et al. (1994)	0.164	14.8	42
	PANI	Richard B. Kaner (1997)	0.174	9.1	43
PANI/PI blend	PANI/polyimide	Richard B. Kaner (1997)	0.282	10	43
	BTDA/ODA	Richard B. Kaner (1997)	0.174	6.2	43
	6FDA-DABA-25	Eva Marand (2002)	12.9	4.76	44
	6FDA−TAPOB	Yasuharu Yamada (2004)	2.25	6.21	45
nondopable polyimide (NDPI)	(BADBSBF−BTDA)	Soon-Ki Kwon (2005)	18	9	46
	6FDA−NDA	Tai Shung Chung (2009)	8.99	5.18	47
	TMPA−6FDA	L. M. Robeson (1999)	122	3.43	48
	6FDA−MDA	Maria Coleman (2010)	0.86	5.3	49
dopable polyimide (DPI)	DPI	this work	1.06	13.54	–
	DPI-doped	this work	0.93	16.63	–

Figure 5b shows the SEM chloride mapping image on the DPI-doped membrane, in which we see many white spots (i.e., the chloride element) dispersed uniformly in a black background (i.e., the polymer matrix), but the white spots essentially disappear in the DPI matrix (Figure 5a). Compared with the DPI membrane, a new element (Cl) appears in the DPI-doped membrane in the EDX spectra, as shown in Figure 5, parts c and d. These results indicate the DPI can be easily doped with HCl and the chloride dopant counterions can be well dispersed in the DPI-doped matrix.

If the material is crystalline in nature, the peak from the X-ray diffraction (XRD) is sharp and the intensity is strong. However, when the material is amorphous, the peak is rather broad. In this study, the present NDPI, DPI, DPI-doped, PANI, and PANI-doped membranes, were all regarded as rather amorphous materials, as can be seen in the XRD patterns in Figure 6A. However, the XRD pattern of an amorphous polymer is typically dominated by one broad peak associated with the center-to-center chain distance or *d*-spacing. The *d*-spacing values were calculated from Bragg's equation, $n\lambda = 2d \sin \theta$, where θ is the angle for a peak in the patterns. Here, 2θ at the maximum intensity appearing at around 14°−24° was used to calculate the *d*-spacing, which was representative of the average degree of openness within the material. The 2θ of the NDPI was around 14.44 Å and the *d*-spacing was about 6.13 Å. After the doping treatment, the 2θ and *d*-spacing values were unchanged because the NDPI could not be doped. Interestingly, upon doping with 1 M HCl (aq), the *d*-spacing of the DPI and PANI membranes decreased from 5.69 to5.02 Å and 4.73 Å to 3.75 Å, respectively. The results indicated that the HCl dopant causes a decrease of *d*-spacing between the center-to-center chain distances. It is believed that polymers with smaller *d*-spacing generally tend to have a smaller fractional free volume (FFV).[32]

The FFV can be calculated by the following equation[33]

$$\mathrm{FFV} = \frac{V - V_0}{V}$$

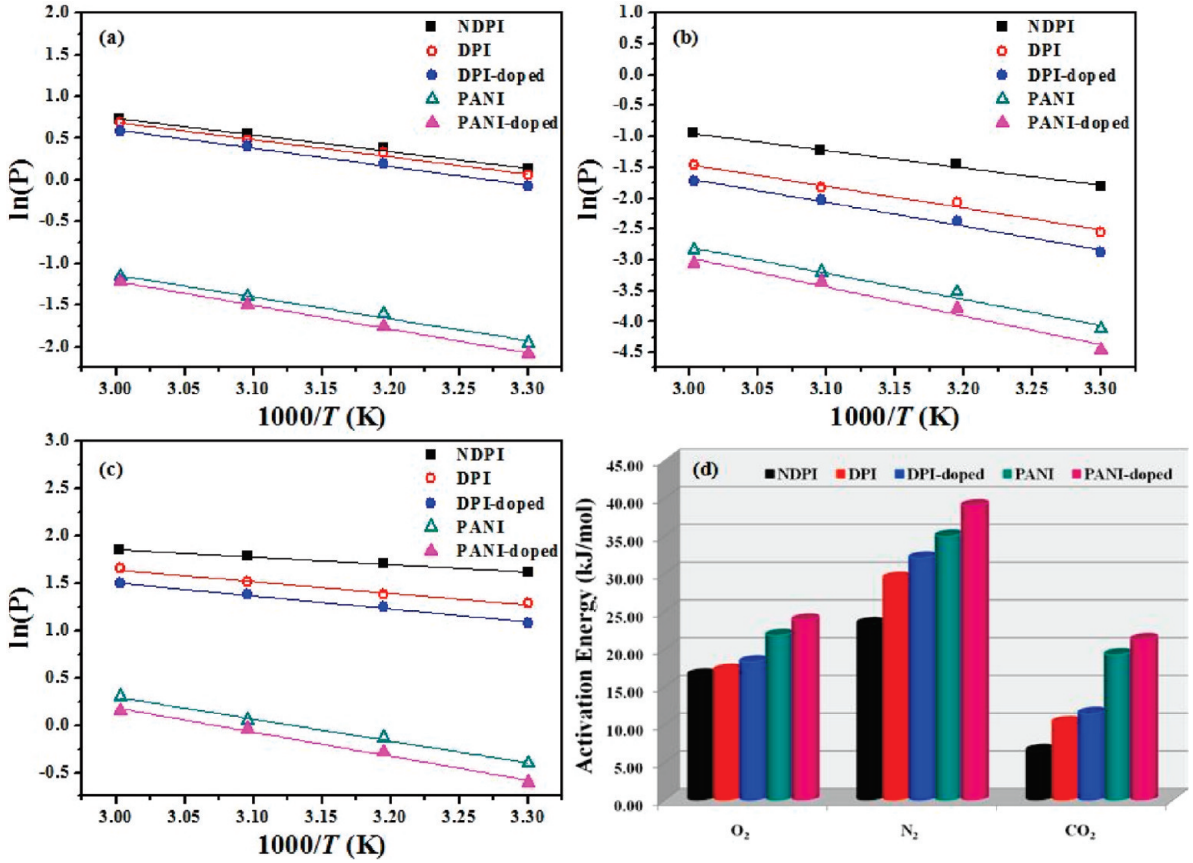

Figure 9. Effect of temperature on the performance of as−prepared membranes: Arrhenius plot of the permeation of (a) O_2, (b) N_2, and (c) CO_2. (d) Activation energy values for the studied membranes.

Table 3. Thermal Properties and Mechanical Strength of NDPI, DPI, and PANI

	thermal properties	mechanical properties		
sample code	T_d[a] (°C)	storage modulus (MPa)	tan δ[b] (°C)	thickness (μm)
NDPI	547	2008	281	50
DPI	593	2800	299	49
PANI	462	1800	228	51

[a] As measured by TGA (onset point). [b] As measured by DMA at 30 °C.

where V is the specific volume and V_0 is the occupied volume of the polymer. The occupied volume was calculated by[34]

$$V_0 = 1.3V_w$$

where V_W is the van der Waals volume which was estimated by the group contribution method by Bondi[34] for the copolymers, the V_w is calculated by $V_W = m_1V_{W1} + m_2V_{W2}$, where m_1 and m_2 are the molar fractions and V_{W1} and V_{W2} refer to the Van der Waals volumes of the homopolyaniline.[34] The specific free volume V_{fmix} is calculated by using the addition method ($V_{fmix} = w_1V_{f1} + w_2V_{f2}$, where w_1 and w_2 are the weight fractions, and V_{f1} is the specific free volume of homopolymers). The obtained ρ and FFV of the specimens are listed in Table 1. The FFV of polymer membranes in this study was calculated to be in the range of 0.056−0.152 and the ordering of DPI-doped > PANI-doped > DPI > NDPI > PANI agreed with the density value. It is worth noticing that the FFV values of DPI decreased from 0.133 to 0.112 while the DPI was doped with 1 M $HCl_{(aq)}$. This phenomenon was similar to PANI results listed in the literature.[11] The decreased FFV can be attributed to the presence of chloride dopant counterions, which fill much of the free volume in the DPI structure.

In general, the performance of membrane units in the separation of a gaseous mixture is highly dependent on the intrinsic physicochemical characteristics of the polymeric materials utilized. The most important properties that need to be taken into account when selecting a polymeric membrane material are (i) its gas permeability and selectivity coefficients, (ii) its mechanical properties, and (iii) its thermal properties.

The permeability coefficients of O_2, N_2, and CO_2 for DPI, NDPI, and PANI membranes were investigated by performing permeation tests at different operational temperatures, as shown in Figure 7 and listed in S-Table 1 (see Supporting Information). The permeability coefficients of corresponding samples for three gases decreased at each temperature, in the order $P(CO_2) > P(O_2) > P(N_2)$. This was also the order of increasing kinetic molecular diameters (CO_2, 3.30 Å; O_2, 3.46 Å; and N_2, 3.64 Å) of the penetrant gases. It was observed that the permeability of NDPI and DPI was higher than that of PANI. Generally speaking, chemical structures coupled with subtle physical properties of the membrane material could influence the permeability and selectivity of a gas. The responses of a polymeric material to permeation are strongly influenced by the polarity and steric

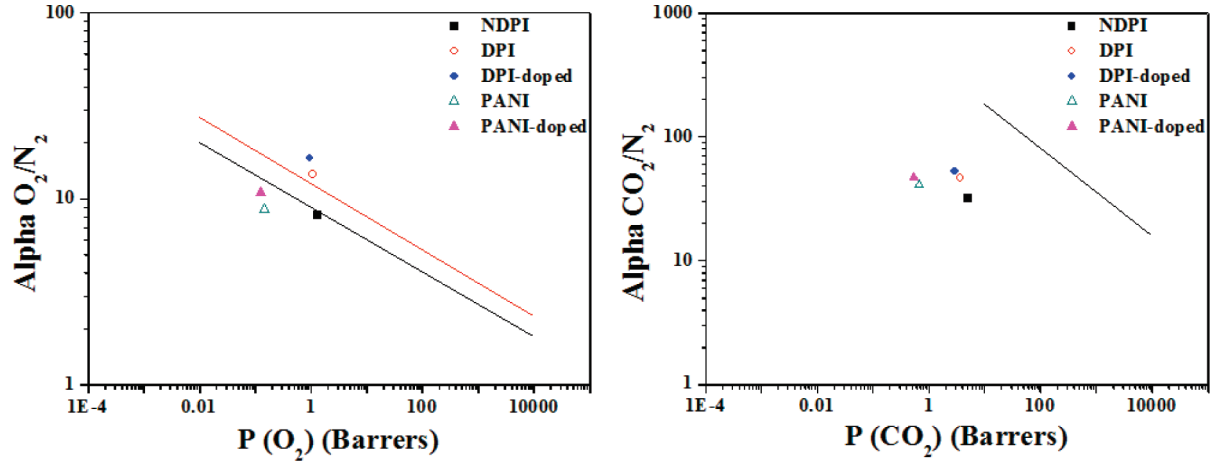

Figure 10. Comparison of the NDPI, PANI, and DPI with a traditional Robeson plot for systems (a) O_2/N_2 and (b) CO_2/N_2.

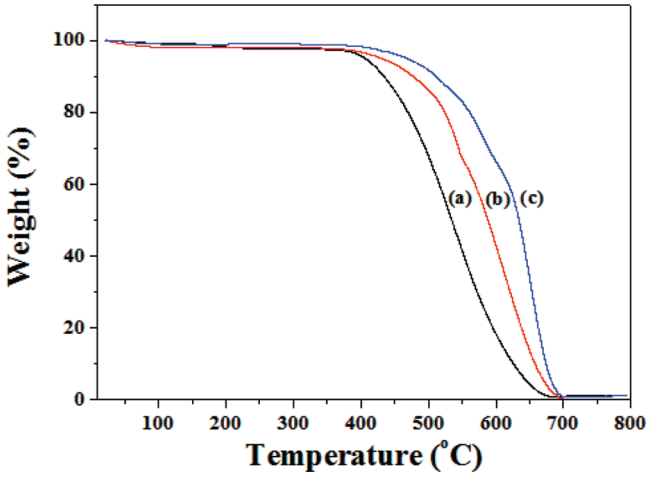

Figure 11. TGA thermograms for (a) PANI (b) NDPI, and (c) DPI.

characteristics of both the polymer and the permeate. The size and shape of bulky groups in both polymer backbones and side chains determine certain fundamental properties like packing density and rigidity, which in turn influence permeability. These parameters, along with the diffusion coefficient, governs the separating capabilities of polymers for O_2, N_2, and CO_2 gas pairs. As polymer molecular spacing becomes tighter the permeability decreases due to decreasing diffusion coefficients but the separation characteristics are enhanced. In this work, polyimide systems contained either rigid (ODA or ACAT) or flexible blocks (BSAA). Rigid block segments provided the main structural framework and better thermal resistance, while the flexible block governed the transportation of gas molecules. On the other hand, PANI consisting of a fully rigid aromatic structure has a higher packing density than polyimide systems. After doping protonic dopants (e.g., 1.0 M HCl) to imide nitrogen on either PANI or DPI backbones, the permeability decreased for all the gases. This effect was due to doping DPI or PANI, in which the dopant reduced the free volume in the polymer (morphological changes) and led to an obvious decrease in gas permeability.[11,12]

Permselectivity of the as-prepared membranes was calculated as the ratio of permeability coefficients of each gas pair, as shown in Figure 8. The temperature dependence of permeability was evaluated and the effect of temperature on the permeability coefficient is listed in S-Table 2 (see Supporting Information). The permselectivity decreased as the temperature increased. With an increase in temperature, the chain mobility and the frequency of intersegmental jumps of gas molecules increased, increasing the diffusion rate as the permeation rate also increased. At the same time, the chain segment motions may have widened, resulting in low selectivity for a gas pair.

We observed that the permselectivity of DPI was greater than it was in the PANI and NDPI membranes, especially in selectivity of O_2/N_2. For example, the permselectivity measured at an operational temperature of 303 K for DPI, NDPI, and PANI was found to be 13.54, 6.89, and 8.76, respectively. It is worth noting that the permselectivity of DPI was on the order of 1.96- and 1.54-fold higher than that of NDPI and PANI, respectively. Upon doping with 1.0 M HCl aqueous for 15 h, the permselectivity of the DPI obviously increased from 13.54 to 16.63, making it almost 2.4-fold higher than that of NDPI. Figure 9 and S-Table 3 (see Supporting Information) present an Arrhenius plot of permeation of O_2, N_2, and CO_2 for all as-prepared samples at an operational pressure of 294 kPa upstream pressure. In general, the temperature dependencies of P can be described by the Arrhenius equation[35]

$$P = P_0 \exp\left(\frac{-E_P}{RT}\right)$$

where P_0 represents pre-exponential factors, E_P is the apparent activation energy for gas permeation, R is the gas constant, and T is temperature. Figure 9d shows the calculated apparent activation energies of O_2, N_2, and CO_2 for permeation and the corresponding pre-exponential factors based on the Arrhenius plots. It can be seen that the activation energy of permeability, E_P, increased with an increase in the kinetic diameter of a penetrant gas and was in the order of CO_2 (3.30 Å), O_2 (3.46 Å), and N_2 (3.64 Å). Although, permeability coefficients increased with temperature, permselectivity for gas pairs of O_2/N_2 and CO_2/N_2 decreased due to differences in permeation activation energies for various gas pairs. Dependence of permselectivity for a gas pair can be evaluated by the difference in activation energy.[36] The DPI exhibited much higher permselectivity than PANI and NDPI, ascribed to the fact that DPI has a much greater difference between N_2 and O_2 in activation energies of permeability, ΔE_P, than PANI and NDPI.

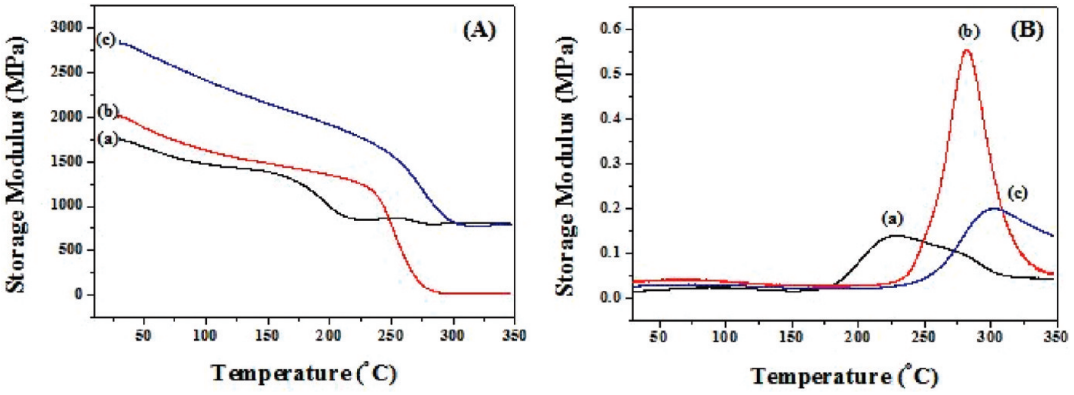

Figure 12. (A) Storage modulus of dynamic mechanical analysis for (a) PANI, (b) NDPI, and (c) DPI. (B) Tan δ of dynamic mechanical analysis for (a) PANI, (b) NDPI, and (c) DPI.

Permselectivity of O_2/N_2 of the as-prepared DPI presented in this study is compared and summarized in Table 2, which includes data proposed by other investigators for free-standing films of PANI and conventional PI. In this study, permselectivity of O_2/N_2, which was about 13.54 for the undoped DPI membrane, was quite comparable to that of PANI and conventional PI film as reported by other investigators[11,37−49] who reported O_2/N_2 permeability selectivity in the range of 2−10. However, upon doping with 1.0 M $HCl_{(aq)}$, the permselectivity of O_2/N_2 of the DPI membrane increased from 13.54 to 16.63.

Polymeric membranes generally undergo a trade-off limitation between permeability and selectivity: as selectivity increases, permeability decreases, and vice versa. Robeson,[50] collecting a large number of permeation data for different polymeric membranes, showed that for small gaseous molecules (e.g., O_2, N_2, and CO_2) a superior limit (upper bound) exists in a selectivity/permeability diagram. In this work, DPI for gas pairs were also evaluated and compared to Robeson's upper bound,[50] as shown in Figure 10. The upper bound demarcated the optimum performance of the polymeric membranes, which typically display a trade-off between permeability and permselectivity. As depicted in Figure 10, the N_2/O_2 separation performances of DPI, NDPI, and PANI displayed a typical trade-off relationship between permeability and permselectivity. The NDPI and PANI permselectivities were lower than those of the DPI and fell below Robeson's old upper bound (1991). Surprisingly, the DPI with doping had a permselectivity that was much higher than Robeson's new upper bound (2008)

An enhancement of the thermal stability behavior of the as-prepared membranes was determined by thermal gravimetric analysis (TGA) under air atmosphere, as shown in Figure 11 and summarized in Table 3. It should be noted that the decomposition temperature (T_d) of DPI was found to be 593 °C, which was significantly higher than that of PANI (about 462 °C) and NDPI (about 547 °C). The dynamic mechanical properties of DPI, NDPI, and PANI films are presented in Figure 12A and are also summarized in Table 3. Specifically, the DPI membrane exhibited storage modulus at about 2800 MPa, which was found to be larger than that of NDPI (about 2008 MPa) and PANI (about 1800 MPa) at room temperature of about 30 °C. At an elevated temperature of about 350 °C, the DPI membrane had a remarkable increase of modulus compared to NDPI and PANI. For as-prepared membranes, the maximum tan δ (E''/E') is defined as the glass transition temperature (T_g).[51] NDPI and PANI were found to show lower glass transition temperatures (T_g) compared with DPI, as shown in Figure 12B. Enhanced mechanical and thermal properties for as-prepared DPI membrane as compared to those of NDPI membrane prepared from similar thermal imidization reactions might be attributed to the incorporated aromatic rigid structure of ACAT into the PI membrane.

CONCLUSIONS

In conclusion, we present the first preparation of an intrinsically dopable polyimide (DPI) membrane containing an amine-capped aniline trimer (ACAT) that reveals advanced gas separation capabilities as well as mechanically and thermally enhanced properties. In regard to gas separation, the permeability and permselectivity of the DPI membrane can be tuned by doping with a dopant. This doping behavior is similar to PANI. Compared with a conventional nondopable PI (NDPI) and PANI, the DPI has good permselectivity about 1.5-fold higher than PANI and 2-fold higher than NDPI. Upon doping with 1.0 M HCl (aq), the permselectivity of DPI was about 2.4-fold higher than that of NDPI. In regard to physical properties, DPI has excellent thermal stability and mechanical properties similar to NDPI. Comparing the mechanical properties of the NDPI and PANI membranes, the DPI membrane showed a storage modulus of 2800 MPa at 30 °C, which was an increase of about 39.4% and 55.5% higher than that of NDPI and PANI membranes, respectively. The decomposed temperature of DPI also increased substantially, to around 131 °C as compared with PANI and to around 46 °C as compared with NDPI. The DPI has good thermal stability, mechanical properties, and high permselectivity, characteristics which might be very useful in the gas separation field.

ASSOCIATED CONTENT

Supporting Information. ^1H NMR and ^{13}C NMR spectra of dopable polyimide model compound, ^1H NMR spectra of dopable polyimide, gas permeability of NDPI, DPI, and PANI, ideal separation factors, and activation energies for DPI, NDPI, and PANI membranes. This material is available free of charge via the Internet at http://pubs.acs.org.

AUTHOR INFORMATION

Corresponding Author

*E-mail: juiming@cycu.edu.tw. Telephone: +886-3-2653340. Fax: +886-3-2653399.

REFERENCES

(1) Koros, W. J. *Macromol. Symp.* **2002**, *188*, 13.
(2) Maier, G. *Angew. Chem., Int. Ed.* **1998**, *37*, 2960.
(3) Stern, S. A. *J. Membr. Sci.* **1994**, *94*, 1.
(4) Freeman, B. D.; Pinnau, I. *Polymer membranes for gas and vapor separations*; ACS Symposium Series 733; American Chemical Society: Washington DC, 1999; Chapter 1.
(5) Caro, J.; Noack, M.; Kölsch, P.; Schäfer, R. *Microporous Mesoporous Mater.* **2000**, *38*, 3.
(6) Chung, T. S.; Jiang, L. Y.; Li, Y.; Kulprathipanja, S. *Prog. Polym. Sci.* **2007**, *32*, 483.
(7) Saufi, S. M.; Ismail, A. F. *Carbon* **2004**, *42*, 241.
(8) Uemiya, S. *Sep. Purif. Methods* **1999**, *28*, 51.
(9) Yampolskii, Y.; Alentiev, A.; Bondarenko, G.; Kostina, Y.; Heuchel, M. *Ind. Eng. Chem. Res.* **2010**, *49*, 12031.
(10) Weber, J.; Du, N.; Guiver, M. D. *Macromolecules* **2011**, *44*, 1763.
(11) Anderson, M. R.; Mattes, B. R.; Heiss, H.; Kaner, R. B. *Science* **1991**, *252*, 1412.
(12) Anderson, M. R.; Mattes, B. R.; Heiss, H.; Kaner, R. B. *Synth. Met.* **1991**, *41*−*43*, 1151.
(13) Pulyalina, A. Y.; Polotskaya, G. A.; Kalyuzhnaya, L. M.; Saprykina, N. N.; Sushchenko, I. G.; Meleshko, T. K.; Toikka, A. M. *Polym. Sci. Ser. A* **2010**, *52*, 856.
(14) Pulyalina, A. Y.; Polotskaya, G. A.; Suschenko, I. G.; Meleshko, T. K.; Kalyuzhnaya, L. M.; Toikka, A. M. *Desalin. Water Treat.* **2010**, *14*, 158.
(15) Chatzidaki, E. K.; Favvas, E. P.; Papageorgiou, S. K.; Kanellopoulos, N. K.; Theophilou, N. V. *Eur. Polym. J.* **2007**, *43*, 5010.
(16) Yorifuji, D.; Ando, S. *Macromolecules* **2010**, *43*, 7583.
(17) Ishizaka, T.; Ishigaki, A.; Chatterjee, M.; Suzuki, A.; Suzuki, T. M.; Kawanami, H. *Chem. Commun.* **2010**, *46*, 7214.
(18) Wang, Z. Y.; Yang, C.; Gao, J. P.; Lin, J.; Meng, X. S.; Wei, Y.; Li, S. *Macromolecules* **1998**, *31*, 2702.
(19) Huang, K. Y.; Jhuo, Y. S.; Wu, P. S.; Lin, C. H.; Yu, Y. H.; Yeh, J. M. *Eur. Poly. J.* **2009**, *45*, 485.
(20) Weng, C. J.; Huang, J. Y.; Huang, K. Y.; Jhuo, Y. S.; Tsai, M. H.; Yeh, J. M. *Electrochimi. Acta.* **2010**, *55*, 8430.
(21) Chao, D.; Lu, X.; Chen, J.; Zhao, X.; Wang, L.; Zhang, W.; Wei, Y. *J. Polym. Sci., Part A: Polym. Chem.* **2006**, *44*, 477.
(22) Chao, D.; Ma, X.; Lu, X.; Cui, L.; Mao, H.; Zhang, W.; Wei, Y. *Macromol. Chem. Phys.* **2007**, *208*, 658.
(23) Chao, D.; Zhang, J.; Liu, X.; Lu, X.; Wang, C.; Zhang, W.; Wei, Y. *Polymer* **2010**, *51*, 4518.
(24) Huang, K. Y.; Shiu, C. L.; Wu, P. S.; Wei, Y.; Yeh, J. M.; Li, W. T. *Electrochim. Acta* **2009**, *54*, 5400.
(25) Weng, C. J.; Chang, C. H.; Peng, C. W.; Chen, S. W.; Yeh, J. M.; Hsu, C. L.; Wei, Y. *Chem. Mater.* **2011**, *23*, 2075.
(26) Miwa, T.; Okabe, Y.; Ishida, M. *Polymer* **1997**, *38*, 4945.
(27) Shacklette, L. W.; Wolf, J. F.; Gould, S.; Baughman, R. H. *J. Chem. Phys.* **1988**, *88*, 3955.
(28) Chen, R.; Benicewic, B. C. *Macromolecules* **2003**, *36*, 6333.
(29) Guo, Y.; Mylonakis, A.; Zhang, Z.; Lelkes, P. I.; Levon, K.; Li, S.; Feng, Q.; Wei, Y. *Macromolecules* **2007**, *40*, 2721.
(30) Li, X.; Wang, G.; Li, X. *Surf. Coat. Technol.* **2005**, *197*, 56.
(31) Zhu, Y.; Zhang, J.; Zheng, Y.; Huang, Z.; Feng, L.; Jiang, L. *Adv. Funct. Mater.* **2006**, *16*, 568.
(32) Huang, S. H.; Hu, C. C.; Lee, K. R.; Liaw, D. J.; Lai, J. Y. *Eur. Polym. J.* **2006**, *42*, 140.
(33) Suzukia, T.; Yamada, Y.; Tsujita, Y. *Polymer* **2004**, *45*, 7167.
(34) Bondi, A. *J. Phys. Chem.* **1964**, *68*, 441.
(35) Pauly, S. In *Polymer Handbook*; Brandrup, J., Immergut, E. H., Grulke, E. A., Eds.; John Wiley: New York, 1999; Vol. 6, p 543.
(36) (a) Lin, W. H.; Chung, T. S. *J. Membr. Sci.* **2001**, *186*, 183. (b) de Sales, J. A.; Patrício, P. S. O.; Machado, J. C.; Silva, G. G.; Windmöller, D. *J. Membr. Sci.* **2008**, *310*, 129.
(37) Illing, G.; Hellgardt, K.; Schonert, M.; Wakeman, R. J.; Jungbauer, A. *J. Membr. Sci.* **2005**, *253*, 199.
(38) Wang, H. L.; Mattes, B. R. *Synth. Met.* **1999**, *102*, 1333.
(39) Lee, Y. M.; Ha, S. Y.; Lee, Y. K.; Suh, D. H.; Hong, S. Y. *Ind. Eng. Chem. Res.* **1999**, *38*, 1917.
(40) Chang, M. J.; Liao, Y. H.; Myerson, A. S.; Kwei, T. K. *J. Appl. Polym. Sci.* **1996**, *62*, 1427.
(41) Rebattet, L.; Escoubes, M.; Genies, E.; Pineri, M. *J. Appl. Polym. Sci.* **1995**, *57*, 1595.
(42) Kuwabata, S.; Martin, C. R. *J. Membr. Sci.* **1994**, *91*, 1.
(43) Su, T. M.; Ball, I. J.; Conklin, J. A.; Huang, S. C.; Larson, R. K.; Nguyen, S. L.; Lew, B. M.; Kaner, R. B. *Synth. Met.* **1997**, *84*, 801.
(44) Cornelius, C. J.; Marand, E. *J. Membr. Sci.* **2002**, *202*, 97.
(45) Suzuki, T.; Yamada, Y.; Tsujita, Y. *Polymer* **2004**, *45*, 7167.
(46) Kim, Y. H.; Kim, H. S.; Kwon, S. K. *Macromolecules* **2005**, *38*, 7950.
(47) Low, B. T.; Chung, T. S.; Chen, H. M.; Jean, Y. C.; Pramoda, K. P. *Macromolecules* **2009**, *42*, 7042.
(48) Robeson, L. M. *Curr. Opin. Solid State Mater. Sci.* **1999**, *4*, 549.
(49) Iyer, P.; Iyer, G.; Coleman, M. *J. Membr. Sci.* **2010**, *358*, 26.
(50) Robeson, L. M. *J. Membr. Sci.* **2008**, *320*, 390.
(51) Chiang, P. C.; Whang, W. T.; Tsai, M. H.; Wu, S. C. *Thin Solid Films* **2004**, *447*, 359.